Reconstitution of β-adrenergic regulation of $Ca_V1.2$: Rad-dependent and Rad-independent protein kinase A mechanisms

Moshe Katz[a], Suraj Subramaniam[b], Orna Chomsky-Hecht[b], Vladimir Tsemakhovich[a], Veit Flockerzi[c], Enno Klussmann[d], Joel A. Hirsch[b,e], Sharon Weiss[a], and Nathan Dascal[a,e,1]

[a]Sackler School of Medicine, Tel Aviv University, Tel Aviv 6997801, Israel; [b]Faculty of Life Sciences, Tel Aviv University, Tel Aviv 6997801, Israel; [c]Experimentelle und Klinische Pharmakologie und Toxikologie, Universität des Saarlandes, 66421 Homburg, Germany; [d]Max Delbrück Center for Molecular Medicine in the Helmholtz Association, 13125 Berlin, Germany; and [e]Sagol School of Neuroscience, Tel Aviv University, Tel Aviv 6997801, Israel

Edited by Kurt G. Beam, University of Colorado Denver, Anschutz Medical Campus, Aurora, CO, and approved April 20, 2021 (received for review January 2, 2021)

L-type voltage-gated $Ca_V1.2$ channels crucially regulate cardiac muscle contraction. Activation of β-adrenergic receptors (β-AR) augments contraction via protein kinase A (PKA)–induced increase of calcium influx through $Ca_V1.2$ channels. To date, the full β-AR cascade has never been heterologously reconstituted. A recent study identified Rad, a $Ca_V1.2$ inhibitory protein, as essential for PKA regulation of $Ca_V1.2$. We corroborated this finding and reconstituted the complete pathway with agonist activation of β1-AR or β2-AR in *Xenopus* oocytes. We found, and distinguished between, two distinct pathways of PKA modulation of $Ca_V1.2$: Rad dependent (∼80% of total) and Rad independent. The reconstituted system reproduces the known features of β-AR regulation in cardiomyocytes and reveals several aspects: the differential regulation of post-translationally modified $Ca_V1.2$ variants and the distinct features of β1-AR versus β2-AR activity. This system allows for the addressing of central unresolved issues in the β-AR–$Ca_V1.2$ cascade and will facilitate the development of therapies for catecholamine-induced cardiac pathologies.

calcium channel | adrenergic | heterologous | protein kinase A | cardiac

Cardiac excitation–contraction coupling crucially depends on the L-type voltage-dependent Ca^{2+} channel, $Ca_V1.2$. Influx of extracellular Ca^{2+} via $Ca_V1.2$ triggers Ca^{2+} release from the sarcoplasmic reticulum via the Ca^{2+} release channel (1). Activation of the sympathetic nervous system increases heart rate, relaxation rate and contraction force. The latter is largely due to increased Ca^{2+} influx via $Ca_V1.2$ (2, 3). Pathological prolonged sympathetic activation progressively impairs cardiac function, causing heart failure, partly due to misregulation of $Ca_V1.2$ (4, 5).

Cardiac $Ca_V1.2$ is a heterotrimer comprising the pore-forming subunit α_{1C} (∼240 kDa), the intracellular $Ca_V\beta_2$ (∼68 kDa) and the extracellular α2δ (∼170 kDa) (Fig. 1*A*) (6, 7). The N and C termini (NT, CT respectively) of α_{1C} are cytosolic and vary among $Ca_V1.2$ isoforms. Further, most of the cardiac α_{1C} protein is posttranslationally cleaved at the CT, around amino acid (a.a.) 1800, to produce the truncated ∼210-kDa α_{1C} protein and the ∼35-kDa cleaved distal CT (dCT); however, the full-length protein is also present (8–11).

The sympathetic nervous system activates cardiac β-adrenergic receptors (β-AR), primarily β1-AR (which is coupled to G_s, is globally distributed in cardiomyocytes, and mediates most of the β-AR-enhancement of contraction and $Ca_V1.2$ activity) and β2-AR, which can couple to both G_s and G_i (12). The cascade of adrenergic modulation of $Ca_V1.2$ comprises agonist binding to β-ARs, activation of G_s and adenylyl cyclase, elevated intracellular cAMP levels, and activation of protein kinase A (PKA) by cAMP-induced dissociation of its catalytic subunit (PKA-CS) from the regulatory subunit. However, the final step, how PKA-CS enhances $Ca_V1.2$ activity, remained enigmatic. A long-standing paradigm was a direct phosphorylation by PKA-CS of α_{1C} and/or $Ca_V\beta$ subunits (3, 13–16). However, numerous studies critically challenged this theory. In particular, mutated $Ca_V1.2$ channels in genetically engineered mice lacking putative PKA phosphorylation sites on α_{1C} and/or β_{2b}, were still up-regulated by PKA (9, 17–21) (reviewed in refs. 6 and 22).

One significant obstacle in deciphering the mechanism of PKA regulation of $Ca_V1.2$ was a recurrent lack of success in reconstituting the regulation in heterologous systems, which proved challenging and controversial (23). Studies in heterologous cellular models, including *Xenopus* oocytes, demonstrated that cAMP failed to up-regulate $Ca_V1.2$ containing the full-length α_{1C}, $Ca_V1.2$-α_{1C} (24–26). However, robust β-AR–induced up-regulation of Ca^{2+} currents was observed in oocytes injected with total heart RNA (27, 28), suggesting the necessity of an auxiliary protein, the "missing link" (24, 25). Interestingly, partial regulation was observed with dCT-truncated α_{1C} (16, 29). Intracellular injection of cAMP or PKA-CS in *Xenopus* oocytes caused a modest (30 to 40%) up-regulation of $Ca_V1.2$, containing a dCT-truncated α_{1C}, $Ca_V1.2$-$\alpha_{1C}\Delta1821$ (29). This regulation required the presence of the initial segment of the long-NT of α_{1C} but did not involve $Ca_V\beta$ subunit. We proposed that this mechanism might account for part of the adrenergic regulation of $Ca_V1.2$ in the heart (29). Normally adrenergic stimulation in cardiomyocytes increases the Ca^{2+}

Significance

The strengthening of heart contraction by epinephrine (adrenaline) and norepinephrine starts with the activation of β-adrenergic receptors and culminates in a protein kinase A–mediated increase in Ca^{2+} influx through the voltage-gated Ca^{2+} channel, $Ca_V1.2$, into cardiomyocytes. Many crucial molecular details of this vital physiological regulation remained enigmatic for decades, not the least owing to the difficulty of reconstituting the regulation in model cells. Capitalizing on the recent discovery of the central role of the $Ca_V1.2$-associated protein, Rad, we present a report of full reconstitution of the β-AR–$Ca_V1.2$ cascade in a model system, the *Xenopus* oocyte, and investigate crucial aspects of regulation such as the roles of auxiliary subunits and diverse forms of the channel protein.

Author contributions: M.K., V.F., E.K., J.A.H., S.W., and N.D. designed research; M.K., S.S., O.C.-H., and V.T. performed research; V.F. contributed new reagents/analytic tools; M.K., S.S., S.W., and N.D. analyzed data; and M.K., S.W., and N.D. wrote the paper.

The authors declare no competing interest.

This article is a PNAS Direct Submission.

[1]To whom correspondence may be addressed. Email: dascaln@tauex.tau.ac.il.

This article contains supporting information online at https://www.pnas.org/lookup/suppl/doi:10.1073/pnas.2100021118/-/DCSupplemental.

Published May 17, 2021.

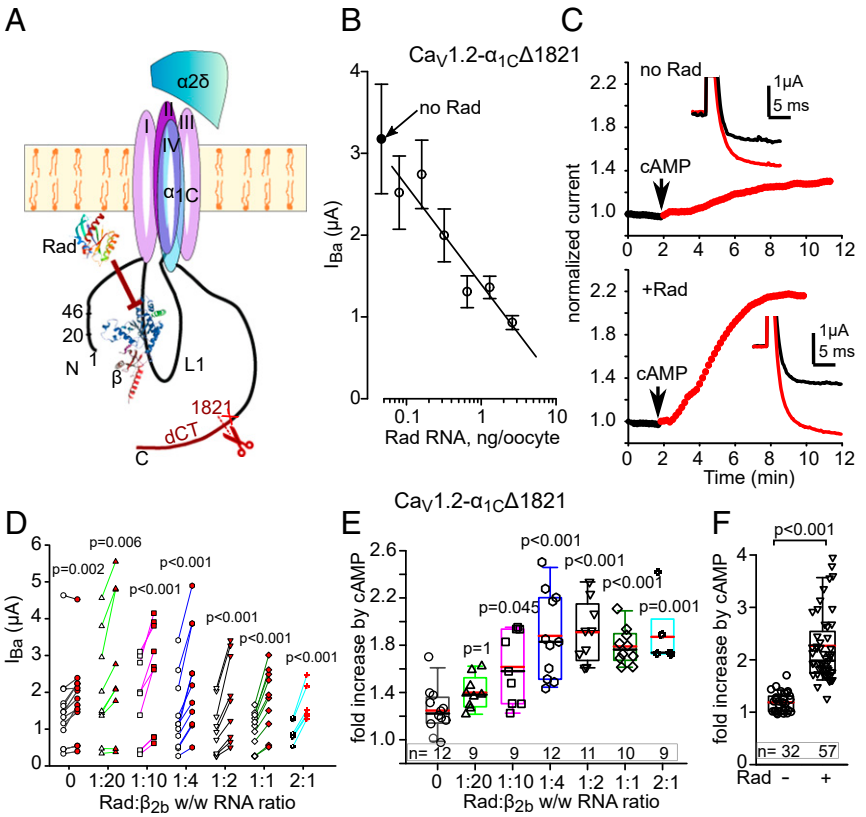

Fig. 1. cAMP regulation of $Ca_V1.2$ is enhanced by coexpression of Rad. (*A*) $Ca_V1.2$ and Rad. α_{1C} and $\alpha2\delta$ subunits are shown schematically, with structures of β_{2b} (38) and Rad (74). The truncation in $\alpha_{1C}\Delta1821$ was at a.a. 1,821 (red cross mark) similar to naturally truncated cardiac α_{1C}, ~a.a. 1800 (9). $Ca_V\beta$ binds to the cytosolic loop I, L1, that connects repeat domains I and II. Rad exerts inhibitory action on the channel, in part through an interaction with $Ca_V\beta$. (*B*) Rad reduces the Ba^{2+} current of $Ca_V1.2$-$\alpha_{1C}\Delta1821$ ($\alpha_{1C}\Delta1821$, β_{2b} and $\alpha2\delta$; 1.5 ng RNA of each subunit) in a dose-dependent manner. Pearson correlation, $r = -0.82$, $P = 0.023$. Each point represents mean ± SEM from 7 to 10 oocytes recorded during 1 d. The linear regression line was drawn for nonzero doses of Rad. (*C*) Rad enhances the cAMP-induced increase in I_{Ba}. Diary plots of the time course of change in I_{Ba} (normalized to initial I_{Ba}) are shown before and after intracellular injection of cAMP in representative cells. No Rad: *Upper*; with Rad: *Lower*. (*Insets*) Currents at +20 mV before (black trace) and 10 min after cAMP injection (red trace). (*D*) "before–after" plots of cAMP-induced changes in I_{Ba} in individual cells injected Rad RNA while varying Rad:β_{2b} RNA ratio (by weight, wt/wt). Empty symbols–before cAMP; red-filled–after cAMP. $n = 3$ experiments; statistics: paired *t* test. (*E*) cAMP-induced increase in I_{Ba} at different Rad/β_{2b} RNA levels (summary of data from *D*). Each symbol represents fold increase in I_{Ba} induced by cAMP injection in one cell. Here and in the following figures, box plots show 25 to 75 percentiles, whiskers show the 5/95 percentiles, and black and red horizontal lines within the boxes are the median and mean, respectively. At all Rad:β_{2b} RNA ratios except 1:20, the cAMP-induced increase in I_{Ba} was significantly greater than without Rad (Kruskal–Wallis test; H = 36.1, 6 degrees of freedom, $P < 0.001$). (*F*) Summary of cAMP effects in 10 experiments without and with Rad at 1:2 and 1:1 Rad:β_{2b} RNA ratios (pooled). Number of cells: within the bars. Statistics: Mann–Whitney *U* test; U = 19.0, $P < 0.001$.

current two- to threefold; thus, a major part of the regulation has remained unexplained.

Recently, Liu et al. identified Rad as the "missing link" in PKA regulation of $Ca_V1.2$ (20). Rad is a member of the Ras-related GTP-binding protein subfamily (RGK) that inhibit high voltage-gated calcium channels Ca_V1 and Ca_V2 (30). Rad tonically inhibits $Ca_V1.2$, largely via an interaction with $Ca_V\beta$ (31, 32). Ablation of Rad in murine heart was shown to increase basal $Ca_V1.2$ activity and rendered the channel insensitive to β-AR regulation, probably through a "ceiling" effect (33, 34). Liu et al. (20) reconstituted a major part of the $Ca_V1.2$ regulation cascade, initiated by forskolin-activated adenylyl cyclase in mammalian cells, ultimately attaining an approximately twofold increase in Ca^{2+} current. The regulation required phosphorylation of Rad, the presence of $Ca_V\beta$, and the interaction of $Ca_V\beta$ with the cytosolic loop I of α_{1C}, suggesting that PKA phosphorylation of Rad reduces its interaction with $Ca_V\beta$ and relieves the tonic inhibition of $Ca_V1.2$ (20, 35).

Importantly, the complete adrenergic cascade, starting with β-AR activation, has not yet been heterologously reconstituted for $Ca_V1.2$. Also, the relation between the Rad-dependent regulation and the regulation reported in our previous study (29) is not clear. Here, we utilized the *Xenopus* oocyte heterologous expression system and successfully reconstituted the entire β-AR cascade. We demonstrate two distinct pathways of PKA modulation of $Ca_V1.2$ (Rad dependent and Rad independent) and characterize the roles of NT and CT of α_{1C}, β_{2b}, and Rad in the adrenergic modulation of cardiac $Ca_V1.2$ channels. Reproducing the complete β-AR cascade in a heterologous expression system will promote the identification and characterization of intracellular proteins that regulate the cascade, eventually assisting efforts to develop therapies to treat heart failure and other catecholamine-induced cardiac pathologies.

Results

Rad Plays a Significant Role in PKA Regulation of $Ca_V1.2$. We used the *Xenopus* oocyte model because of its two major advantages: the ability to coexpress a large number of proteins and control over protein expression in a wide range (by titrated RNA injection). There are limitations similar to other heterologous models. Expression of a protein may change the levels of the others; the relation between injected RNA and the expressed protein is not necessarily linear. Still, the control of protein expression is better than for DNA introduction into mammalian cells by transfection or viral infection. These limitations can be overcome through precise

monitoring of protein expression levels and RNA dose readjustment (e.g., ref. 36).

In *Xenopus* oocytes, PKA regulation of heterologously expressed $Ca_V1.2$ was previously observed only with dCT-truncated but not full-length α_{1C}wt (2171 a.a. long) (24, 29). Therefore, we started the study of Rad's role in regulation of $Ca_V1.2$ using α_{1C} truncated at a.a. 1821, $\alpha_{1C}\Delta1821$. We expressed $Ca_V1.2$ in full subunit composition, $\alpha_{1C}\Delta1821$, β_{2b}, and α2δ, at a 1:1:1 RNA ratio (by weight). Without Rad coexpression, I_{Ba} was increased by 19 ± 3% ($n = 32$, $P = 0.002$) following cAMP injection (Fig. 1 *C*–*F*). This is less than the previously reported 30 to 40% (29), probably because here, we injected about half the amount of cAMP. Note that a greater Rad-independent I_{Ba} potentiation was attained by injecting purified PKA-CS (*SI Appendix*, Fig. S2).

Next, we tested the effect of increasing Rad concentrations by varying the amount of Rad RNA. I_{Ba} was measured by voltage steps from −80 to +20 mV (refer to Fig. 1*C*, *Insets* for examples of I_{Ba} recordings). As expected (31, 37), basal I_{Ba} was reduced by expression of Rad, showing an inverse correlation with Rad RNA dose (Fig. 1*B*). Importantly, coexpression of Rad dramatically augmented the effect of cAMP (Fig. 1 *C* and *E*). This effect of Rad increased with increasing doses of injected Rad RNA, becoming statistically significant at Rad:β_{2b} RNA ratios above 1:10 and reaching a maximum at 1:2 Rad:β_{2b} RNA ratio (Fig. 1*E*). The average increase at 1:1 and 1:2 RNA ratios was more than twofold (127 ± 10%, $n = 57$; Fig. 1*F*).

Rad-Dependent and Rad-Independent Regulations Are Distinct: Roles of β Subunit and NT and CT of α_{1C}. Experiments in human embryonic kidney (HEK) cells suggested a crucial role for the $Ca_V\beta$ subunit in Rad-dependent PKA regulation of $Ca_V1.2$ (20, 35). To further evaluate the role of $Ca_V\beta$, we compared the change in I_{Ba} following injection of cAMP into oocytes expressing $\alpha_{1C}\Delta1821$ and α2δ, without $Ca_V\beta$ or with β_{2b}-wt (wild type), β_{2b}-core (38), or

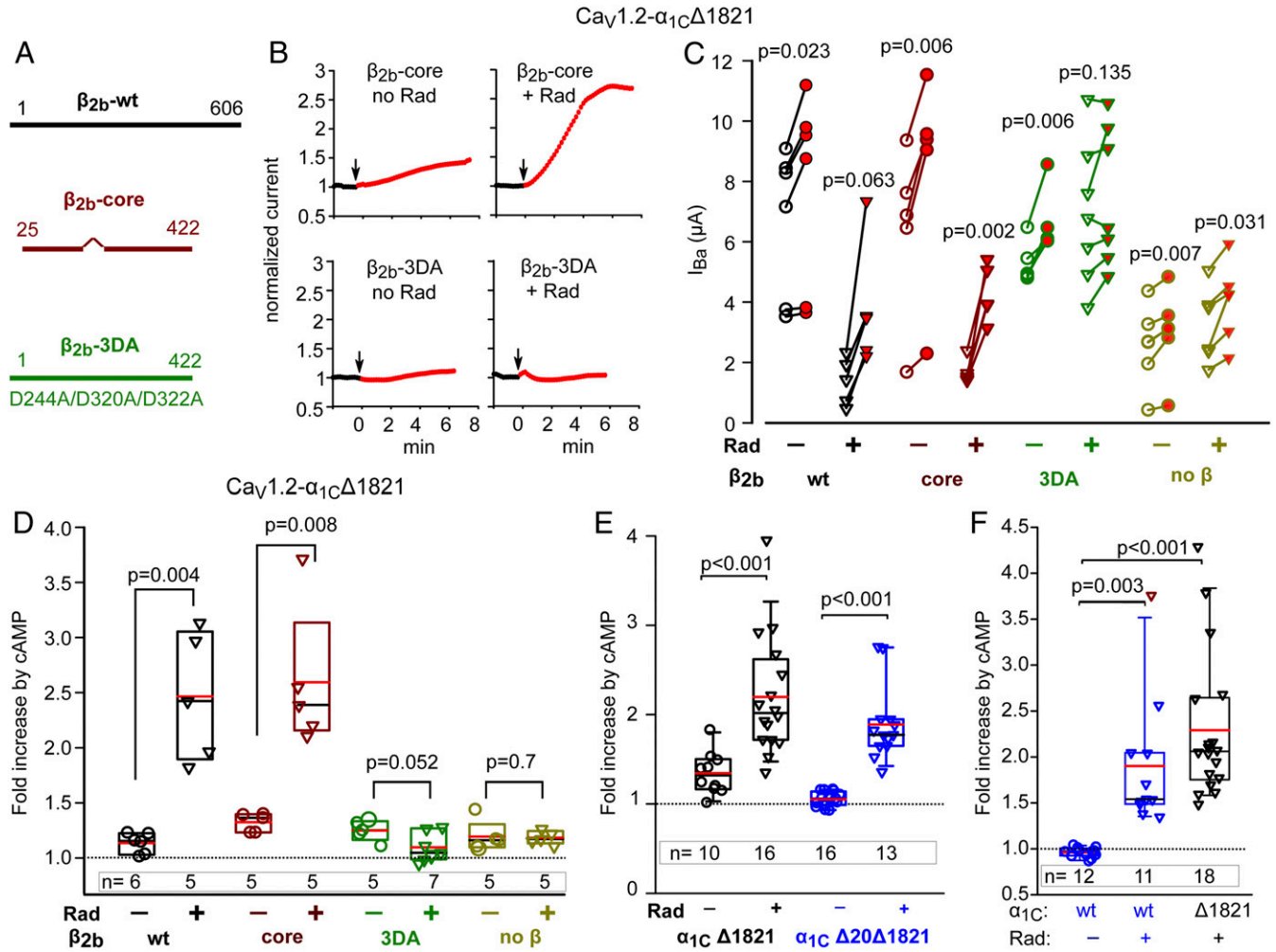

Fig. 2. Separation of Rad-dependent and Rad-independent PKA regulation of α_{1C}. In all experiments, Rad:β_{2b} RNA ratio was 1:2 or 1:1. (*A*) Schematic representation of $Ca_V\beta$ variants used. The wild-type (β_{2b}-wt) protein is 606 a.a. long. β-core was truncated at a.a. 422; the linker a.a. 138 to 202 were removed (38). The β_{2b}-3DA is the β_{2b} truncated at a.a. 422, with three Asp-to-Ala mutations, D244A/D320A/D322A. (*B*–*D*) the presence of the β subunit and its ability to bind Rad are crucial for Rad-dependent but not for Rad-independent cAMP regulation of $Ca_V1.2$. 1 experiment. (*B*) Diary plots of cAMP-induced changes in I_{Ba} (see *SI Appendix*, Fig. S1 for additional examples). (*C*) Before–after plots of cAMP-induced changes in I_{Ba}. Statistics: paired *t* test. (*D*) Summary of data from *C*. Data show the fold increase with Rad coexpression (inverted triangles) and without Rad (circles). Groups with and without Rad were compared by Mann–Whitney *U* Rank Sum test (*t* test for β_{2b}-3DA groups in which normality was satisfied). (*E*) The role of N-terminal initial segment of α_{1C}. Data shown are cAMP-induced changes in I_{Ba} in individual cells expressing $Ca_V1.2$-$\alpha_{1C}\Delta1821$ (black) and $Ca_V1.2$-$\alpha_{1C}\Delta20\Delta1821$ (red; the latter is lacking the first 20 a.a. of the N terminus), with α2δ and β_{2b}, without or with Rad. Refer to *SI Appendix*, Fig. S1*B* for raw data. Three experiments; statistics: Mann–Whitney *U* test. (*F*) The role of dCT of α_{1C}. Data show the fold increase in I_{Ba} after cAMP injection (raw data are shown in *SI Appendix*, Fig. S1 *C* and *D*). Cells expressed the full length α_{1C} (α_{1C}wt) or $\alpha_{1C}\Delta1821$, α2δ and β_{2b}, without or with Rad. Three experiments; statistics: Kruskal–Wallis test; H = 27.017 with 2 degrees of freedom, $P = <0.001$.

β_{2b}-3DA, with or without Rad (Fig. 2*A*). β_{2b}-3DA was designed on the basis of C-terminally truncated β_{2b} and contained the triple mutation D244A/D320A/D322A which abolishes $Ca_V\beta$-Rad association (37, 39).

In the absence of Rad, cAMP induced the typical 20 to 30% increase in I_{Ba} with all β_{2b} constructs or without $Ca_V\beta$ expression (Fig. 2 *B–D* and *SI Appendix*, Fig. S1*A*). In the presence of coexpressed Rad, cAMP induced a much larger, ~2.5-fold increase in peak currents when β_{2b}-wt or β_{2b}-core were expressed but only a small increase in I_{Ba} when no $Ca_V\beta$ or the β_{2b}-3DA mutant was expressed (Fig. 2 *B–D* and *SI Appendix*, Fig. S1*A*). The latter residual increase resembled the cAMP effect seen without Rad. These results suggest that there are two separate cAMP-induced regulations of $Ca_V1.2$ in *Xenopus* oocytes. A mild 20 to 30% increase that does not depend on the presence of $Ca_V\beta$ (29) and does not require coexpression of Rad is termed hereafter "Rad-independent." The larger, approximately twofold cAMP-induced increase in I_{Ba} requires the expression of exogenous Rad and will be termed "Rad-dependent" PKA regulation. Absence of $Ca_V\beta$ or abrogation of the β_{2b}-Rad interaction eliminates the Rad-dependent PKA regulation of $Ca_V1.2$, confirming that Rad-dependent PKA regulation of $Ca_V1.2$ is $Ca_V\beta$

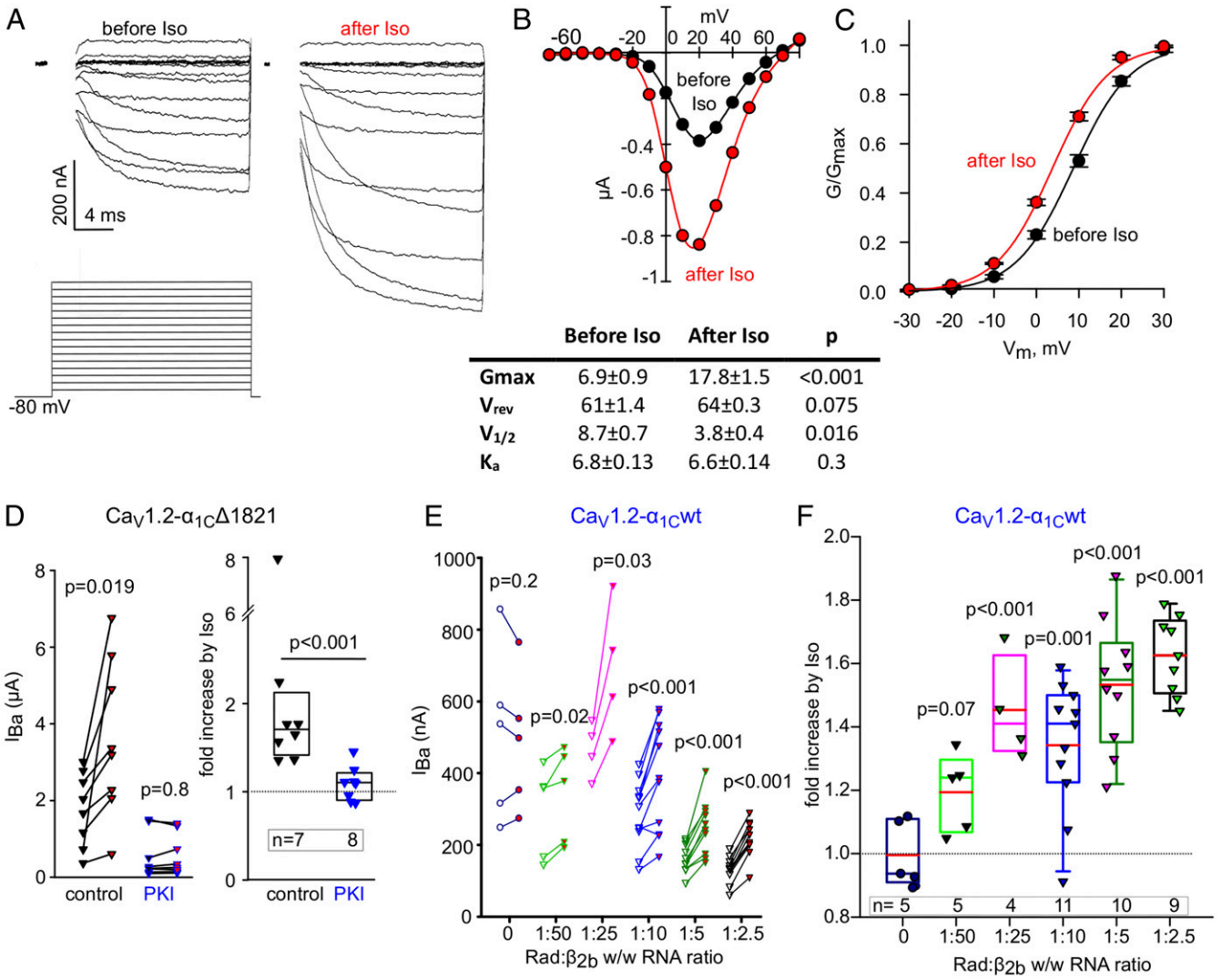

Fig. 3. Full reconstitution of the β1-AR regulation of $Ca_V1.2$. (*A–C*) β1-AR regulation of voltage-dependent activation of $Ca_V1.2$. Oocytes were injected with RNA of $\alpha_{1C}\Delta1821$, α2δ, β_{2b}, Rad, and β1-AR. (*A*) Ba^{2+} currents (*Upper*) before (*Left*) and after (*Right*) perfusion of 50 µM isoproterenol (Iso) in a representative cell. The voltage protocol is illustrated in the *Lower* panel; I_{Ba} was elicited by 20 ms voltage steps given every 10 s from a holding potential of −80 mV in 10 mV increments. The currents shown are net I_{Ba} derived by subtraction of the residual currents recorded with the same protocols after applying 200 µM Cd^{2+}. Since full capacity, compensation in oocytes was not achievable, and the currents during the first ~2 ms (the duration of capacity transient) were blanked out. (*B*, *Top*) I–V curve before (black) and after (red) addition of Iso in the oocyte shown in *A*. (*Bottom*) Parameters of Boltzmann fit of I–V curves in seven oocytes, before and after Iso. (*C*) Conductance–voltage (G–V) curves of $Ca_V1.2$-$\alpha_{1C}\Delta1821$ coexpressed with Rad and β1-AR averaged from oocytes of a representative batch ($n = 7$ oocytes, one experiment) before and after Iso. The curves were drawn using the Boltzmann equation using average $V_{1/2}$ and K_a obtained from the fits of I–V curves in individual oocytes (from the table shown in *B*, *Bottom*). (*D*) PKI protein blocks the Iso-induced increase in I_{Ba}. Cells expressed $\alpha_{1C}\Delta1821$, α2δ, β_{2b}, Rad, and β1-AR. Purified PKI protein (29) was injected to a final concentration of ~2 µM assuming oocyte volume of 1 µL, 0.5 to 2 h before measuring the currents. Control, no PKI preinjection. (*Left*) Before–after plots; statistics: paired *t* test. (*Right*) Summary of data from one experiment (Mann–Whitney *U* Rank Sum Test). (*E* and *F*) β1-AR regulation of $Ca_V1.2$-α_{1C}wt with increasing doses of Rad RNA. α2δ, β_{2b}, and β1AR were coexpressed in all groups. (*E*) Before–after plots of Iso-induced changes in I_{Ba}, at increasing doses of Rad RNA. One experiment; statistics: paired *t* test. (*F*) Fold change increase in I_{Ba} caused by Iso as a function of Rad:β_{2b} RNA ratio. Summary of the experiment shown in *E*. Statistics: one-way ANOVA, $F = 11.8$, $P < 0.001$.

dependent. β_{2b}-core is sufficient to mediate the regulation. This indicates that the variable $Ca_V\beta_2$ NT and CT and part of its HOOK domain are not required for the Rad inhibition of the channel nor for the relief of inhibition following phosphorylation of Rad by PKA.

Next, we examined the roles of NT and dCT, which are highly important for the Rad-independent regulation (29). The predominant cardiac isoform is the long-NT α_{1C} in which the first 46 a.a. are encoded by exon 1a (40, 41) (*SI Appendix*, Fig. S2*A*). The first 20 a.a. of the cardiac long-NT α_{1C} isoform act as an inhibitory module, tonically reducing the open probability and currents of $Ca_V1.2$ (42). Removal of this module ($\alpha_{1C}\Delta20\Delta1821$) abrogates most of the Rad-independent cAMP regulation of $\alpha_{1C}\Delta1821$ in oocytes (ref. 29 and Fig. 2*E* and *SI Appendix*, Fig. S1*B*). We further validated the importance of this inhibitory module by replacing by alanine of either the conserved a.a. T_{10}, Y_{13}, and P_{15} (TYP motif) or a.a. 2 to 5 (α_{1C}NT-TYP$\Delta1821$ and α_{1C}NT-4A$\Delta1821$ mutants, respectively). These mutations suppress the inhibitory function of the NT module (42). We now show that they also abrogate the PKA-CS regulation of a mouse $Ca_V1.2$ in the absence of Rad (*SI Appendix*, Fig. S2 *B–D*), confirming the crucial role of the NT initial segment in the Rad-independent regulation. In contrast, the Rad-dependent regulation was preserved in $\alpha_{1C}\Delta20\Delta1821$ (Fig. 2*E* and *SI Appendix*, Fig. S1*B*). Thus, unlike the Rad-independent regulation, the Rad-dependent regulation does not require an intact NT inhibitory module.

The cleaved dCT of α_{1C} subunit is a potent inhibitory domain (43) that can reassociate with the truncated α_{1C}, forming a tight molecular complex (10). The cleaved dCT was proposed to be essential for PKA regulation of $Ca_V1.2$ (3, 16). In addition, the cleaved dCT has been reported to traffic to the nucleus in which it serves as a transcription regulator (44, 45). However, in *Xenopus* oocytes, the presence of dCT as a separate protein was not required for Rad-independent regulation of $Ca_V1.2$-$\Delta1821$ (29). Forskolin up-regulated $Ca_V1.2$ in HEK cells coexpressing Rad and full-length (wt) $Ca_V1.2$ channels, $Ca_V1.2$-α_{1C}wt (20). All in all, the role of dCT and its truncation in Rad-dependent regulation remains incompletely understood.

To examine the role of dCT, we first compared the effect of cAMP on either full-length (wt) α_{1C} or $\alpha_{1C}\Delta1821$-containing channels, in the absence and presence of Rad. Coexpression of Rad (1:3 to 1:1 Rad:β_{2b} RNA ratio) reduced basal currents of $Ca_V1.2$-α_{1C}wt, with median I_{Ba} of 3.05 μA without Rad and 0.62 μA with Rad ($P < 0.001$; *SI Appendix*, Fig. S1*D*). Injection of cAMP into cells expressing wt-α_{1C} did not increase I_{Ba} (actually, a slight reduction of 4 ± 1.5%, $n = 12$, was observed: Fig. 2*F* and *SI Appendix*, Fig. S1 *C* and *D*). In contrast, when Rad was coexpressed with wt-α_{1C}, cAMP injection strongly increased I_{Ba} (by 90 ± 21%, $n = 11$, $P = 0.003$) (Fig. 2*F* and *SI Appendix*, Fig. S1 *C* and *D*). Thus, unlike Rad-independent regulation, Rad-dependent PKA regulation does not require the cleavage of dCT.

Interestingly, in the same experiments, the Rad-dependent cAMP-induced increase in I_{Ba} appeared higher in oocytes coexpressing Rad with $\alpha_{1C}\Delta1821$ (Fig. 2*F*): 128 ± 23%, $n = 18$. Pairwise comparison of fold increase in I_{Ba} for $Ca_V1.2$-α_{1C}wt versus $Ca_V1.2$-$\alpha_{1C}\Delta1821$ showed a mildly significant difference, $P = 0.04$ (Mann–Whitney *U* test, median 2.06 interquartile range [IQR] 1.77 to 2.63 for $\alpha_{1C}\Delta1821$ versus median 1.54 [IQR 1.49–2.04] for wt-α_{1C}).

We also found that dCT, coexpressed as a separate protein, did not affect regulation by cAMP of $Ca_V1.2$-$\alpha_{1C}\Delta1821$ even in the presence of Rad ($P = 0.48$) (*SI Appendix*, Fig. S1 *E* and *F*). Thus, the clipped dCT does not appear to play a role in PKA regulation of the truncated $Ca_V1.2$.

Full Reconstitution of the β1-AR Regulation of $Ca_V1.2$. We report the reconstitution of the full cascade β-adrenergic cascade, starting with activation of β1-AR. We expressed β1-AR and $Ca_V1.2$-$\alpha_{1C}\Delta1821$ with or without Rad. In the presence of Rad, isoproterenol (Iso; 50 μM), a nonselective β-AR agonist (46), elicited a significant increase in I_{Ba}. Fig. 3 shows Ba^{2+} currents (Fig. 3*A*) and the current–voltage relationship (Fig. 3*B*) in a representative oocyte. Fig. 3*C* shows a conductance–voltage (G–V) curve drawn from seven oocytes of the same day's experiment. Iso not only increased current amplitudes but also caused a ~5-mV hyperpolarization shift in the $V_{1/2}$ for activation, without changing the slope factor (Fig. 3 *B*, *Lower*). The Iso-induced increase in I_{Ba} was blocked by the specific PKA inhibitor, the protein kinase inhibitor (PKI) protein (Fig. 3*D*), suggesting that the effect of Iso was mediated by PKA-CS. Without Rad, Iso had no effect on $Ca_V1.2$-$\alpha_{1C}\Delta1821$ (see Fig. 4).

We next examined β1-AR regulation of $Ca_V1.2$-α_{1C}wt (full-length α_{1C}). Titration of Rad expression with variable amounts of RNA showed an inverse correlation between Rad:β_{2b} RNA ratio and I_{Ba} ($r = -0.85$, $P = 0.002$; *SI Appendix*, Fig. S3). Rad dose-dependently enhanced the Iso effect (Fig. 3 *E* and *F*), similar to what we observed with $\alpha_{1C}\Delta1821$, though maximal Rad effect appeared to occur at lower Rad:β_{2b} RNA (Fig. 3*F*, compare with Fig. 1*E*).

We next systematically compared the effect of Iso on channels containing either wt-α_{1C} or $\alpha_{1C}\Delta1821$, with or without coexpressed β1-AR and Rad (Fig. 4 and *SI Appendix*, Fig. S4). Without the coexpression of Rad, activation of β1-AR did not produce any increase in I_{Ba} in either full-length or truncated channel. This result indicates that the Rad-independent pathway is not activated by β1-AR under the conditions used. Moreover, it appears that oocytes do not contain endogenous Rad or similar RGK proteins that are available for the β1-AR–$Ca_V1.2$ cascade. Interestingly, when oocytes expressed Rad without the receptor, Iso caused a small increase in I_{Ba}: ~15% in $\alpha_{1C}\Delta1821$ (which did not reach statistical significance, $P = 0.08$ by paired *t* test) and ~33% in wt-α_{1C} ($P = 0.016$) (Fig. 4). These results corroborate a previous report (47), suggesting that endogenous β-AR is present in some oocyte batches.

In oocytes that expressed β1-AR, Rad, and $Ca_V1.2$, Iso induced a robust increase in I_{Ba} (Fig. 4 *A* and *B*; $P < 0.001$ for both α_{1C} forms). Interestingly, the Iso effect on the truncated channel was greater than on full-length α_{1C} (147% versus 87% increase in mean I_{Ba}, respectively; $P = 0.002$; Fig. 4*B*), similar to what we observed for the cAMP effect (Fig. 2*F*). Thus, in the full-length channel, the dCT seems to attenuate the PKA-induced augmentation of $Ca_V1.2$ currents.

Reconstitution of the β2-AR Regulation of $Ca_V1.2$. β2-AR is localized in specific parts of the heart (atrium, apex) and specifically in T-tubules within cardiomyocytes but becomes more widely distributed over the cardiomyocyte surface in failing heart (4, 48–50). To study β2-AR regulation of $Ca_V1.2$, we expressed β2-AR, Rad, and $Ca_V1.2$-$\alpha_{1C}\Delta1821$, using β2-AR RNA doses between 10 and 200 pg/oocyte (higher RNA doses caused oocyte mortality). Unexpectedly, exposure to Iso did not produce a significant increase in I_{Ba} in oocytes expressing β2-AR, although a clear increase was observed in oocytes of the same batch expressing β1-AR (Fig. 5 *A* and *B*).

To test whether the expressed β2-AR was functioning well, we used cystic fibrosis transmembrane conductance regulator (CFTR) channel, a chloride channel activated by PKA phosphorylation (51). CFTR is robustly activated by cAMP and PKA-CS injection in *Xenopus* oocytes (52, 53). Coexpressing CFTR with a range of β2-AR doses (RNA range, 5 to 50 pg/oocyte) was associated with significantly higher basal chloride currents (I_{CFTR}) compared with cells expressing CFTR alone ($P < 0.001$), and Iso did not further increase I_{CFTR} in β2-AR–expressing oocytes (*SI Appendix*, Fig. S5). We hypothesized that CFTR channels may have already been activated due to the agonist-independent constitutive activity of β2-ARs (54), thus blunting any response to Iso. To test this, we incubated the oocytes for 1 to 2 h with 10 μM propranolol, a β-blocker and an inverse agonist known to reduce the constitutive activity of β2-AR (54). Following propranolol incubation, the oocyte was placed in the experimental chamber, voltage clamp was

PHYSIOLOGY

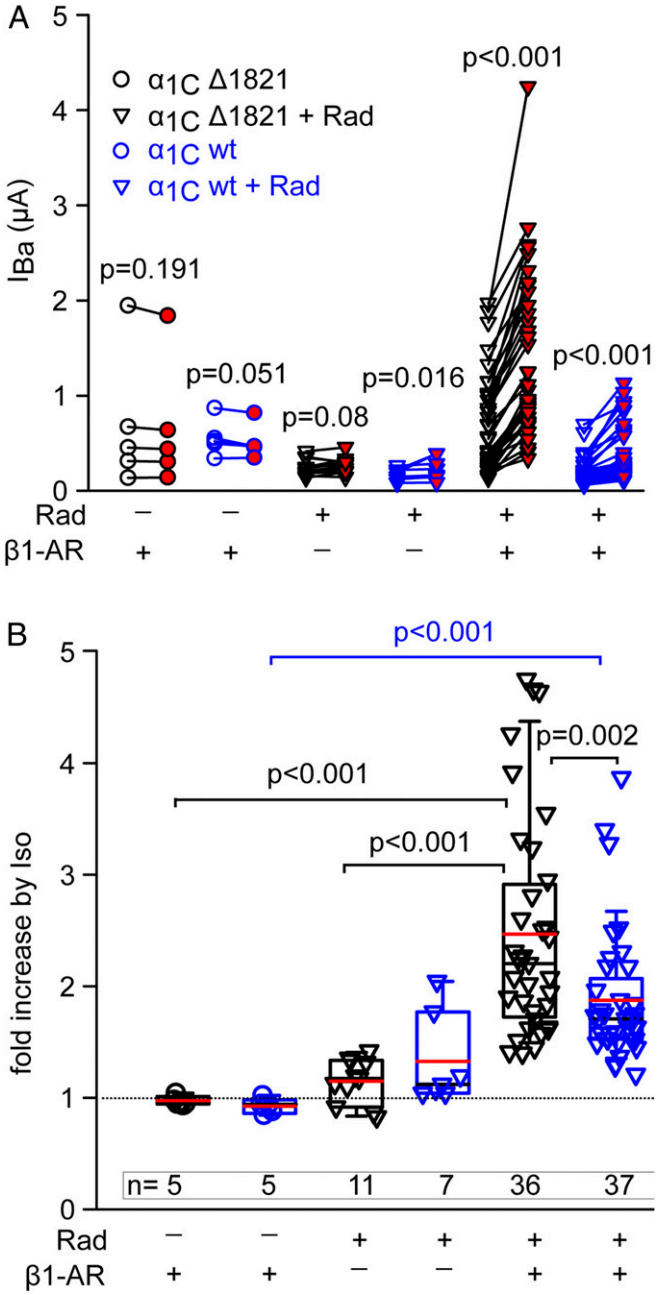

Fig. 4. β1-AR regulation of full-length and truncated α_{1C}. Oocytes expressed $Ca_V1.2$-α_{1C}wt (full-length) or $Ca_V1.2$-α_{1C}Δ1821 channels with or without Rad and β1-AR. (*A*) Before–after plots of Iso-induced changes in I_{Ba} in individual cells. The Rad:β2b RNA ratio in oocytes expressing wt $Ca_V1.2$ (blue symbols) or $Ca_V1.2$Δ1821 (black symbols) was 1:3 and 1:2, respectively. Three experiments; statistics: paired *t* test. (*B*) Summary of experiments shown in *A*. Statistics: ANOVA on ranks, separately for wt $Ca_V1.2$-α_{1C} ($H = 18.2$, $P < 0.001$) and $Ca_V1.2$-α_{1C}Δ1821 ($H = 32.4$, $P < 0.001$). In addition, Mann–Whitney *U* Rank Sum test was used to compare the last two groups, wt $Ca_V1.2$ versus $Ca_V1.2$Δ1821 with Rad and β1-AR ($U = 382$, $P = 0.002$). For $Ca_V1.2$-α_{1C}wt with Rad, there was no significant difference between the groups with and without β1-AR ($P = 0.076$, one-way ANOVA on ranks, Dunnett's test).

established, and the cell was washed with propranolol-free solution for 2 to 4 min before application of Iso. With propranolol preincubation, Iso induced a robust 1.5- to 3-fold increase in CFTR currents (*SI Appendix*, Fig. S5).

These results supported the possibility that high constitutive activity of β2-AR precluded further effect of Iso, also in the case of $Ca_V1.2$. Indeed, preincubation with propranolol resulted in a statistically significant reduction of basal I_{Ba} in oocytes expressing β2-AR, Rad, and $Ca_V1.2$-α_{1C}Δ1821 (Fig. 5*C*). Application of Iso produced a mild but significant increase in I_{Ba} without propranolol incubation, by 24 ± 5%, in this experiment, and significantly greater increase, three to fivefold, with propranolol preincubation (Fig. 5 *D*–*F*).

β2-AR regulation of $Ca_V1.2$ may be especially relevant for the regulation of the full-length α_{1C}, which is present in the heart but is particularly abundant in neurons, in which it is regulated by β2-AR; the prominent PKA phosphorylation site S1928 located in the dCT of α_{1C} has been reported to crucially contribute to this regulation (reviewed in ref. 55). We tested β2-AR regulation of the $Ca_V1.2$-α_{1C}S1928A mutant in which serine 1928 was replaced by alanine (56). Fig. 5 *G* and *H* shows that I_{Ba} was significantly and similarly increased by Iso in both $Ca_V1.2$-α_{1C}wt and $Ca_V1.2$-α_{1C}S1928A, following preincubation with propranolol and washout as above, in cells coexpressing $Ca_V1.2$ and Rad. Thus, phosphorylation of S1928 does not play a major role in Rad-dependent regulation of full-length $Ca_V1.2$ in this reconstitution model.

Brain and smooth muscle express a rich variety of α_{1C} isoforms resulting from alternative splicing (6, 57, 58). The predominant α_{1C} isoforms in the brain and smooth muscle have a short NT initial segment (16 a.a.) encoded by exon 1b (*SI Appendix*, Fig. S2*A*); smooth muscle and a proportion of cardiac channels often contain an insertion in loop I encoded by exon 9* (9a) (58–60). We examined β2-AR regulation of two α_{1C} variants (made on the template of full-length α_{1C}) corresponding to major brain and smooth muscle isoforms, in which the long-NT (46 a.a.) was replaced by short NT (16 a.a.; *SI Appendix*, Fig. S2*A*) without or with the addition of exon 9*-encoded segment in loop I. Fig. 5 *I* and *J* shows that Iso induced a significant and similar two- to 2.5-fold increase in both channel forms. Thus, Rad-dependent β2-AR regulation is preserved in brain- and smooth muscle-like $Ca_V1.2$ variants in this reconstitution model.

Discussion

Reconstitution of numerous regulatory pathways of ion channels in heterologous systems has accelerated the understanding of their mechanisms and structure–function relationships. However, the classical adrenergic regulation of cardiac L-type Ca^{2+} channel remained an unmet challenge for several decades. The recent discovery of the crucial role of Rad and partial reconstitution of the cascade starting from activation of adenylyl cyclase by forskolin (20) was a turning point. Here we report the heterologous reconstitution of the full cascade of β-AR regulation of the cardiac L-type Ca^{2+} channel, $Ca_V1.2$, in *Xenopus* oocytes, starting with the receptor. We utilized the simplicity and robustness of the oocyte expression system to reconstitute the full β-AR cascade, to address the role of Rad, the relation between Rad-dependent and the previously reported Rad-independent PKA regulation (29), and to elaborate the role of $Ca_V\beta$ and the distal parts of NT and CT of α_{1C}.

We first validated the role of Rad by directly activating the endogenous PKA through intracellular injection of cAMP. Titrated expression of Rad showed the expected (31, 32) decrease in I_{Ba} of $Ca_V1.2$-α_{1C}Δ1821, highly correlated with Rad RNA dose and accompanied by a robust enhancement in cAMP-induced increase in I_{Ba}, up to ∼2.2-fold (Fig. 1). This is similar to the ∼1.5- to twofold increase in maximal conductance (G_{max}) of $Ca_V1.2$-α_{1C}wt in Rad-expressing HEK cells by forskolin (20) and the magnitude of the adrenergic effect in cardiomyocytes. These results confirm the importance of Rad in PKA regulation and show that Rad-dependent regulation occurs both in full-length and C-terminally truncated α_{1C}.

cAMP/PKA-CS injection results strongly suggest two mechanistically distinct PKA regulatory modes of $Ca_V1.2$ (Fig. 2 and *SI Appendix*, Figs. S1 and S2): Rad independent and Rad dependent. The latter accounted for ∼80% of total increase in I_{Ba}

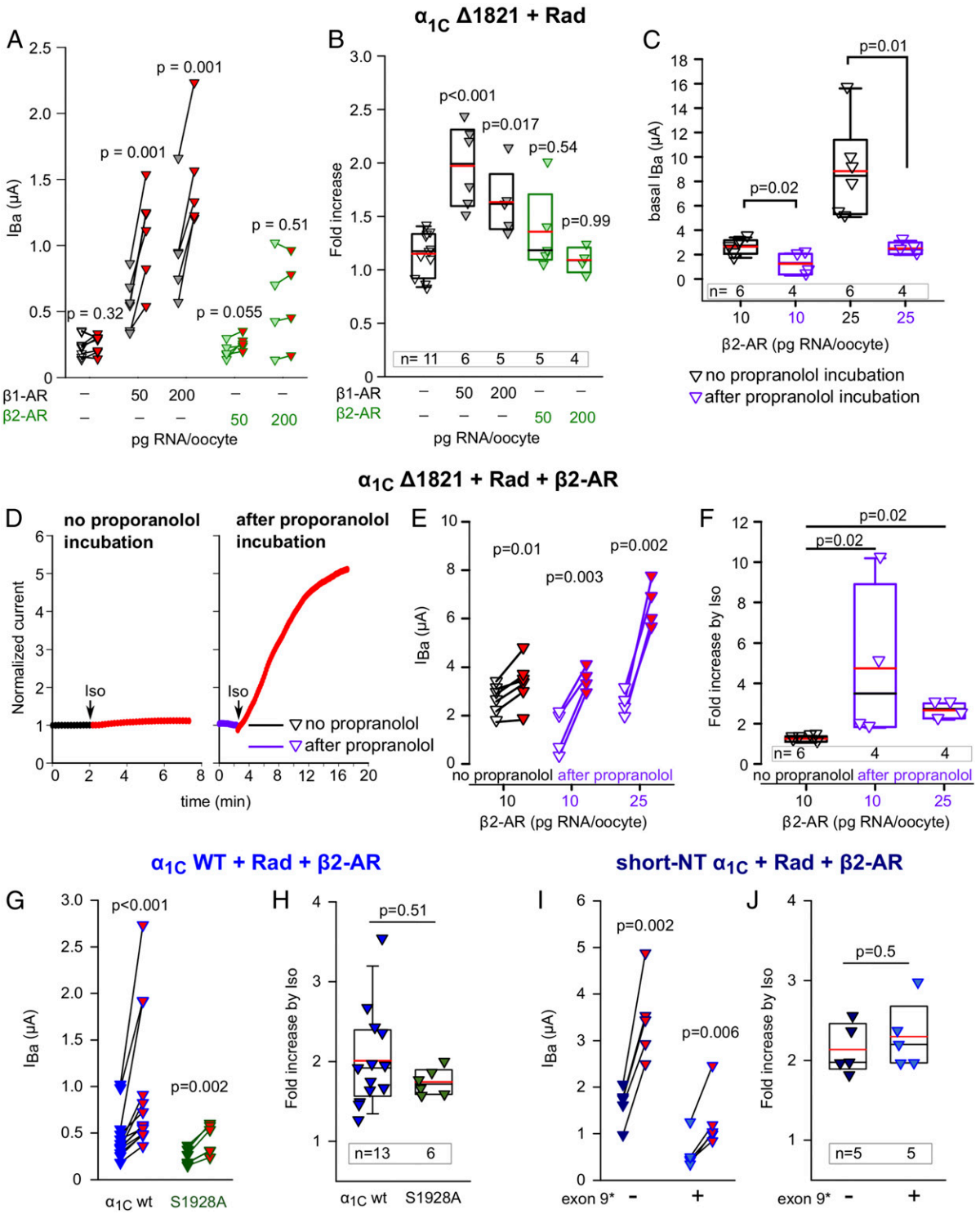

Fig. 5. β2 adrenergic regulation of $Ca_V1.2$. (*A* and *B*) Unlike β1-AR, β2-AR does not up-regulate $Ca_V1.2\Delta1821$ when activated by Iso. Rad:β_{2b} RNA ratio was 1:2. Records were taken from oocytes of the same batch during a 3-d experiment. DNAs of both receptors were in pGEM-HJ vector. (*A*) Before-after plots and (*B*) summary of Iso-induced changes in I_{Ba}, without or with either β1-AR or β2-AR. Statistics: *A*, paired *t* test; *B*, one-way ANOVA ($F = 9.9$, $P < 0.001$) followed by Dunnett's test. (*C*) Basal I_{Ba} of $Ca_V1.2\Delta1821$ is reduced by preincubation with propranolol for 60 to 120 min (10 μM; purple symbols). Rad:β_{2b} RNA ratio was 1:2. One experiment; statistics: *t* test. (*D–F*) Iso regulates $Ca_V1.2$ via β2-AR following reduction in constitutive activity of the receptor by propranolol pre-incubation. Representative diary plots (*D*), Before-after plots (*E*) and summary of Iso-induced increase in oocytes coexpressing $\alpha_{1C}\Delta1821$, Rad, and β2-AR without and with preincubation with propranolol. One experiment, statistics: paired *t* test (*E*), Kruskal–Wallis one-way ANOVA ($H = 9.6$, $P = 0.001$) followed by Dunnett's test (*F*). (*G* and *H*) The S1928A mutation in the distal CT of full-length α_{1C} does not abrogate the β2-AR regulation. Oocytes expressed α_{1C}-WT or α_{1C}-WT S1928A, β_{2b}, α2δ, Rad, and β2-AR and were preincubated in propranolol prior to Iso challenge. Raw data from three experiments are shown in before–after plot (*G*; statistics: paired *t* test) and the summary is in *H* (statistics: Mann–Whitney *U* test). (*I* and *J*) β2-adrenergic regulation of short-NT isoforms of α_{1C}, with or without exon 9*. Oocytes expressed short-NT α_{1C}-wt with or without exon 9*, β_{2b}, α2δ, Rad, and β2-AR and were preincubated in propranolol prior to Iso challenge. Raw data from one experiment are shown in before–after plot (*I*; statistics: paired *t* test), and the summary is in *J* (statistics: *t* test).

when Rad was coexpressed. The first major mechanistic difference is the role of $Ca_V\beta$. The Rad-dependent regulation was fully $Ca_V\beta$ dependent, as shown before (20). Both Rad inhibition of the basal I_{Ba} and the Rad-dependent cAMP enhancement of I_{Ba} critically depended on coexpression of $Ca_V\beta$ subunit (full-length or core), and both Rad actions were suppressed by a triple mutation that abolishes Rad-$Ca_V\beta$ interaction (Fig. 2). The absolute requirement of Rad-dependent regulation for coexpression of $Ca_V\beta$ suggests that endogenous $Ca_V\beta$ present in the oocytes in small amounts (61) is insufficient to support this regulation or cannot couple to coexpressed Rad. In contrast, Rad-independent regulation did not depend on the presence of $Ca_V\beta$ subunit. Second, as shown before (29), the Rad-independent regulation crucially involved two cytosolic elements of α_{1C}: it required truncation of dCT of α_{1C} and the presence of the inhibitory module (initial segment) of the NT (Fig. 2 and *SI Appendix*, Figs. S1 and S2). In contrast, in the presence of Rad, robust regulation of I_{Ba} by cAMP was consistently observed, both after the deletion of the initial NT segment and in channels containing either full-length or dCT-truncated α_{1C}. We conclude that the cAMP/PKA-CS–induced PKA enhancement of $Ca_V1.2$ current, to date observed only in *Xenopus* oocytes (29), is a Rad-independent mode of regulation, distinct from the Rad-dependent one.

We next reconstituted the full β-AR–$Ca_V1.2$ cascade with coexpressed β1-AR or β2-AR. Our results reveal differences between the two receptors and provide insights into the mechanisms of β-AR regulation of $Ca_V1.2$. Activation of β1-AR by Iso caused a greater-than-twofold increase in $Ca_V1.2$-$\alpha_{1C}\Delta1821$ current and the typical hyperpolarizing shift in voltage dependence of activation (Fig. 3), like in cardiomyocytes (21). Coexpression of G_s and adenylyl cyclase was not necessary, suggesting sufficient levels of endogenous proteins. However, expression of Rad was essential for both β1-AR and β2-AR regulation; in its absence, no increase in I_{Ba} was observed (Figs. 3 and 4). Thus, if RGK proteins are present in *Xenopus* oocytes, they are insufficient or unable to support β-AR regulation of $Ca_V1.2$. This result also further underscores the distinction between Rad-dependent and Rad-independent mechanisms. It is unclear why the Rad-independent regulation of $Ca_V1.2$-$\alpha_{1C}\Delta1821$ could not be produced by the activation of β-ARs; it could be a missing specific protein or a stoichiometry problem with either the receptor or a downstream protein of the cascade. Unfortunately, expression of high doses or β1-AR, $G\alpha_s$, or adenylyl cyclase consistently resulted in oocyte mortality. Hence, we concluded that β1-AR regulated $Ca_V1.2$ only via the Rad-dependent mechanism under our experimental conditions.

Our experiments revealed a significant difference in basal activity of β1-AR and β2-AR. As demonstrated with both CFTR and $Ca_V1.2$, even with lowest RNA doses used, β2-AR constitutively activated the G_s-PKA pathway, rendering high basal CFTR and $Ca_V1.2$ currents and precluding further β-AR regulation. Low basal currents and β2-AR regulation of CFTR and $Ca_V1.2$ were restored by preincubation with the inverse β-AR agonist, propranolol (Fig. 5 and *SI Appendix*, Fig. S5). Whereas high basal constitutive activity of β2-AR is well established (54, 62, 63), agonist stimulation of β2-AR normally increases $Ca_V1.2$ currents in the heart (46, 50). We assume that, in cardiomyocytes, specific mechanisms such as restricted localization (4, 11, 49, 50, 64, 65) or additional auxiliary proteins may regulate the basal activity of β2-AR.

The successful reconstitution of both β1-AR and β2-AR regulation of $Ca_V1.2$ allowed an initial testing of several open questions related to $Ca_V1.2$ isoforms and posttranslationally modified variants in brain and smooth muscle. Our data (Fig. 5) show similar β-AR Rad-dependent regulation of cardiac $Ca_V1.2$ and of α_{1C} variants representing predominant neuronal and smooth muscle isoforms, featuring a short N-terminal initial segment and an insertion in loop I encoded by exon 9*. The latter complements the recent finding of Papa et al. (35) who demonstrated unaltered β-AR regulation of $Ca_V1.2$ containing the long N-terminal initial segment and the 9* insertion in loop I, in cardiomyocytes of genetically engineered mice.

We have addressed in detail the role of the posttranslational proteolytic cleavage of dCT of α_{1C} that has been unclear and even controversial (23). Of particular importance is the observation that, in the presence of Rad, both dCT-truncated and full-length channels were up-regulated by cAMP and by β1-AR and β2-AR (Figs. 2, 4, and 5). The full-length α_{1C} is present in the heart and seems even more abundant in neurons, where β2-AR is the predominant β-AR (11). The mechanism of regulation of neuronal $Ca_V1.2$ appears different from that of cardiac; the direct PKA phosphorylation of serine 1928 (located in the dCT) is highly important in neurons and smooth muscle (55, 66, 67), but not in the heart (18, 68). In our system, the β1-AR activation of full-length $Ca_V1.2$ (containing S1928) required Rad, and mutation of S1928 to alanine did not suppress the β2-AR regulation of $Ca_V1.2$-α_{1C}wt. Thus, phosphorylation of S1928 in not required for the Rad-dependent β-AR regulation. However, since both the $Ca_V1.2$ microenvironment and the RGK protein abundance in neurons and cardiomyocytes may substantially differ, involvement of S1928 cannot be ruled out (55). Notably, phosphorylation of S1928 contributes to basal I_{Ba} in the oocytes (56) and modulates mobility of neuronal $Ca_V1.2$ (69), suggesting multiple roles for this prominent PKA site.

Our results did reveal a potentially important quantitative difference that depended on dCT cleavage: in Rad-expressing oocytes, the β1-AR and cAMP regulation of the dCT-truncated channel was significantly stronger than of the full-length channel. Although this could represent the contribution of Rad-independent regulation (which is missing in the full-length channel), we consider this unlikely since Rad-independent regulation was not observed with β1-AR. We propose that, in the context of full-length α_{1C}, the dCT exerts a regulatory control over the Rad-dependent β-AR regulation of the channel, via mechanisms that remain to be explored.

In summary, we reconstituted the β1-AR and β2-AR regulation of $Ca_V1.2$ in the *Xenopus* oocyte model system. Our heterologous model replicates the known basic features of β-AR regulation of cardiac $Ca_V1.2$ and reveals previously unknown molecular details, including the consequences of proteolytic processing of α_{1C} with respect to β-AR regulation, the differential roles of $Ca_V\beta$ subunit and of the NT and CT of α_{1C} in the Rad-dependent and Rad-independent regulation, and the differences in channel regulation by β1-AR and β2-AR. The reconstitution of the basic cascade will enable further investigation of the mechanisms of action of Rad and additional auxiliary proteins implicated in macromolecular complexes involved in β-AR regulation of $Ca_V1.2$, such as arrestins, G protein receptor kinases, A-kinase anchoring proteins, phosphatases and phosphodiesterases, and others (70). It may also be instrumental in identifying potential targets for therapeutic modulation of β-adrenergic regulation in heart and other tissues.

Materials and Methods

Experimental Animals and Ethical Approval. Experiments were approved by Tel Aviv University Institutional Animal Care and Use Committee (permits # 01–16-104 and 01–20-083). Adult female *Xenopus laevis* frogs were purchased from Xenopus 1 (Dexter, MI). The frogs were handled as described (29). For surgery, frogs were anesthetized in 0.2% tricaine methanesulfonate (MS-222). After removal of portions of ovary and full recovery from anesthesia, frogs were returned to a separate tank for postoperational animals. For details, refer to *SI Appendix*.

DNA Constructs, RNA, and Purified Proteins. The complementary DNA (cDNA) constructs used are the following: Human Rad (NP_001122322), cardiac long N terminus isoform of rabbit α_{1C} (GenBank: X15539) and the corresponding mouse α_{1C} isoform (NM_001255999.2), rabbit $Ca_V\beta_{2b}$ [originally termed β_{2a} (71); GenBank: X64297.1; $Ca_V\beta2N4$ according to the comprehensive nomenclature (6)], and $\alpha_2\delta_1$ (GenBank: M21948). Two NT mutants of mouse α_{1C} were constructed: α_{1C}NT-4AΔ1821 with alanine substitution of a.a. 2 to 5

and α_{1C}NT-TYPΔ1821 with alanine substitution of a.a. T_{10}, Y_{13} and P_{15}. Mouse α_{1C} constructs also contained the double mutation T1066Y/Q1070M which renders the channel dihydropyridine insensitive but does not affect regulation by PKA (19). The DNA of the distal C-terminal fragment (dCT) of rabbit α_{1C} encoded a.a. 1,821 to 2,171 (29). The short NT forms of α_{1C}, with and without the insertion of exon 9*-encoded segment of loop L1, were prepared on the template of rabbit α_{1C}wt (42, 72). The β_{2b}-core construct and β_{2b}-3DA were prepared on the template of β_{2b} described by Opatowsky et al. (73) and described in Fig. 2*A* and *SI Appendix, Methods*. Human CFTR channel (GenBank: NM_00492) was in pSP64 vector. Human β2 adrenergic receptor (GenBank: AAA88015.1) was subcloned into pGEM-HJ vector. Mouse β1 adrenergic receptor (NP_031445.2) was in pcDNA3.1 vector. For comparison with β2 adrenergic receptor, it was subcloned into pGEM-HJ vector. For further details, refer to *SI Appendix*.

The RNAs were prepared using a standard procedure (29). We used the long-NT isoform of rabbit α_{1C} (except *SI Appendix*, Fig. S2, in which mouse α_{1C} was used) and various mutants, as detailed in the figures. The amount of injected RNA, per oocyte, are detailed in *SI Appendix, Methods* and figure legends.

His-tagged catalytic subunit of PKA (His-PKA-CS, GenBank: NM 008854.5) and His-tagged human PKI protein (GenBank: S76965.1) were purified from *Escherichia coli* as described (29), with minor modifications for His-PKA-CS. For details, refer to *SI Appendix*. PKI was stored and injected into oocytes in PKI buffer (in millimolars: 20 Tris HCl, 300 NaCl, 2 dithiothreitol (DTT), pH 8). His-PKA-CS was stored and injected in PKA buffer (in millimolars: 20 KH_2PO_4, 20 KCl, 2 DTT, pH 7.5) (29).

Electrophysiology. Oocytes were defolliculated by collagenase, injected with RNA, and incubated for 3 d before recording at 20 to 22 °C in NDE solution (in millimolars: 96 NaCl, 2 KCl, 1 $MgCl_2$, 1 $CaCl_2$, 5 Hepes, 2.5 pyruvic acid, and 0.1 gentamycin sulfate) (29). Ion channel currents in oocytes were measured using two-electrode voltage clamp with a GeneClamp 500 amplifier (Molecular Devices). CFTR currents were measured at −80 mV in ND96 solution (in millimolars: 96 NaCl, 2 KCl,1 $MgCl_2$, 1 $CaCl_2$, 5 Hepes, pH 7.6). Whole-cell Ba^{2+} current (I_{Ba}) was elicited by 20 ms depolarizing pulses from a resting potential of −80 mV to 20 mV, with a 10 s interval between sweeps, in 40 mM Ba^{2+} solution (in millimolars: 40 $Ba(OH)_2$, 50 NaOH, 2 KOH, and 5 Hepes, titrated to pH 7.5 with methanesulfonic acid), or, in one experiment out of the three with α_{1C}Δ20Δ1821 (Fig. 2*E*), in 2 mM Ba^{2+} solution (in millimolars: 2 $Ba[OH]_2$, 96 NaOH, 2 KOH, and 5 Hepes, titrated to pH 7.5 with methanesulfonic acid). These measurements were used to assess cAMP-induced changes in I_{Ba} amplitude only. Experiments with one oocyte batch lasted for 2 to 3 d (3 to 5 d after RNA injection). Channel levels usually increased on days 2 and 3. Therefore, in most experiments, the effects of cAMP and Iso on a Rad-less channel (that exhibited the highest currents) were measured on the first day to avoid measuring too large currents (>8 μA) that caused series resistance artifacts. Effects of various treatments (e.g., different doses of Rad; *SI Appendix*, Figs. S1*B* and S3) on basal I_{Ba} were always compared on the same day, in 40 mM Ba^{2+} solution. Results of "before–after" analysis of single cells (cAMP injection, Iso) were collected during all days of recording. Therefore, generally, the populations of cells used to summarize I_{Ba} amplitude versus cells in which effects of cAMP or Iso were measured only partially overlap.

In the current–voltage (I–V) protocols, currents were elicited by 20 ms pulses from the holding potential −80 mV to voltages from −70 to 80 mV with 10 mV intervals and 10 s between sweeps. Currents measured in the presence of 200 μM Cd^{2+} were subtracted from total I_{Ba} (Fig. 3 *A*–*C*) to yield the net I_{Ba}. I–V curves were analyzed as described (42). In each cell, I–V curves in the range −70 to 40 mV were fitted to the Boltzmann equation in the form:

$$I = G_{max}(V_m\text{-}V_{rev})/(1 + \exp(\text{-}(V_m - V_{1/2})/K_a)),$$

where G_{max} is the maximal Ba^{2+} conductance, V_m is the membrane voltage, V_{rev} is the reversal potential of the current, K_a is the slope factor, and $V_{1/2}$ is half-maximum activation voltage. The parameters obtained for G_{max} and V_{rev} were then used to calculate fractional conductance data points at each V_m using the equation:

$$G/G_{max} = I/(G_{max}(V_m\text{-}V_{rev})).$$

Conductance–voltage (G–V) curves through the data points were plotted with the values of $V_{1/2}$ and K_a obtained from the fit of the I–V curves, using the following form of the Boltzmann equation:

$$G/G_{max} = 1/(1 + \exp(\text{-}V_m\text{-}V_{1/2})/K_a)).$$

Injection of cAMP and PKA-CS and Isoproterenol Perfusion. cAMP (Sigma, A6885) was diluted in H_2O, stored in small aliquots as 40 mM stock solution at −20 °C and thawed only once. For injection, cAMP was diluted to 20 mM. Purified His-PKA-CS was kept in aliquots of 5 μg/μl and stored in small aliquots at −80 °C and thawed at the beginning of the experiment and during the experiment kept on ice. Injection during recording was done with sharp capillary glass micropipettes filled with cAMP or PKA-CS. The injection needle was inserted after the whole-cell voltage clamp has been established. Compounds were injected into oocytes with pressure only after observing that currents have been stable for at least 2 min. Approximately 5 nL (0.5% of oocyte volume) was injected. The concentration of injected cAMP in the oocytes was ∼100 μM, assuming oocyte volume of 1 μL. The final amount of PKA-CS injected was ∼25 ng/oocyte. Injection artifacts visible as a sharp shift in current, accompanied by an increase in leak current, were usually minor (Figs. 1*C* and 2*B*). Records with injection artifact that exceeded 10% of I_{Ba} amplitude were discarded.

Isoprenaline hydrochloride (isoproterenol, Sigma-Aldrich, I5627) was diluted in H_2O and kept in 100 mM stock solution aliquots. Perfusion of isoproterenol 50 μM began after documentation of a stable peak current for 2 min. Propranolol (Sigma-Aldrich, P0844) was in dissolved dimethylsulphoxide (DMSO) at 50 mM. For the propranolol pretreatment procedure, oocytes were incubated for 1 to 2 h in 10 μM propranolol in NDE solution.

Statistical Analysis. In all experiments, the fold change in current caused by an externally applied or injected substance was calculated by dividing the current at the end of the recording by the current measured before substance application in the same cell. The values before and after treatment with cAMP/PKA-CS/Isoproterenol were compared using paired *t* test for normally distributed variables; otherwise, a Wilcoxon test was performed (In the text of the paper, mean values ± SE of mean are occasionally presented even for distributions that did not pass normality tests, for reader's convenience). Two-sample comparisons of different treatment groups were done by independent sample two-tailed *t* test, or by Mann–Whitney *U* test for data that did not pass normality test. Comparison of multiple test groups was done with one-way ANOVA if the data were normally distributed or Kruskal–Wallis ANOVA on ranks when the data did not distribute normally. A Holm–Sidak post hoc test was performed for normally distributed data and Dunnett's post hoc test otherwise. Statistical analysis was performed with SigmaPlot 13 (Systat Software, Inc.). Data sets that did not pass the Shapiro–Wilk normality test were reported as median and IQR (Q1 to Q3). In the figures, box plots show the 25 to 75 percentiles, whiskers show the 5 to 95 percentiles, and black and red horizontal lines within the boxes are the median and mean, respectively, with single values (dots) indicated.

Data Availability. All study data are included in the article and/or *SI Appendix*.

ACKNOWLEDGMENTS. This research was supported by the German–Israeli Science Foundation (Grant I-1452-203.13/2018) to N.D., E.K., V.F., and S.W.; the Gessner Fund to M.K. and N.D.; the Deutsche Forschungsgemeinschaft (Grant DFG KL1415/7-1) and the program project Grant 394046635-SFB 1365 to E.K.; the Deutsche Forschungsgemeinschaft grants to V.F. (FOR 2290, TP P1, SFB 894, TP A3); Israel Science Foundation Grants 1519/12 and 1500/16 to J.A.H.; and a Seymour Fefer grant to M.K. M.K. was supported in part by a scholarship from the Alrov Foundation. S.S. was supported in part by a scholarship from the Prajs–Drimmer Institute at Tel Aviv University.

1. D. M. Bers, Calcium cycling and signaling in cardiac myocytes. *Annu. Rev. Physiol.* **70**, 23–49 (2008).
2. H. Reuter, Calcium channel modulation by neurotransmitters, enzymes and drugs. *Nature* **301**, 569–574 (1983).
3. W. A. Catterall, Regulation of cardiac calcium channels in the fight-or-flight response. *Curr. Mol. Pharmacol.* **8**, 12–21 (2015).
4. J. M. Best, T. J. Kamp, Different subcellular populations of L-type Ca^{2+} channels exhibit unique regulation and functional roles in cardiomyocytes. *J. Mol. Cell. Cardiol.* **52**, 376–387 (2012).
5. S. R. Post, H. K. Hammond, P. A. Insel, β-adrenergic receptors and receptor signaling in heart failure. *Annu. Rev. Pharmacol. Toxicol.* **39**, 343–360 (1999).
6. F. Hofmann, V. Flockerzi, S. Kahl, J. W. Wegener, L-type $Ca_V1.2$ calcium channels: From in vitro findings to in vivo function. *Physiol. Rev.* **94**, 303–326 (2014).
7. A. C. Dolphin, Voltage-gated calcium channels and their auxiliary subunits: Physiology and pathophysiology and pharmacology. *J. Physiol.* **594**, 5369–5390 (2016).
8. T. Gao *et al.*, Identification and subcellular localization of the subunits of L-type calcium channels and adenylyl cyclase in cardiac myocytes. *J. Biol. Chem.* **272**, 19401–19407 (1997).

9. A. Katchman *et al*., Proteolytic cleavage and PKA phosphorylation of α_{1C} subunit are not required for adrenergic regulation of $Ca_V1.2$ in the heart. *Proc. Natl. Acad. Sci. U.S.A.* **114**, 9194–9199 (2017).
10. J. T. Hulme, V. Yarov-Yarovoy, T. W. Lin, T. Scheuer, W. A. Catterall, Autoinhibitory control of the $Ca_V1.2$ channel by its proteolytically processed distal C-terminal domain. *J. Physiol.* **576**, 87–102 (2006).
11. S. Dai, D. D. Hall, J. W. Hell, Supramolecular assemblies and localized regulation of voltage-gated ion channels. *Physiol. Rev.* **89**, 411–452 (2009).
12. R. P. Xiao *et al*., Subtype-specific β-adrenoceptor signaling pathways in the heart and their potential clinical implications. *Trends Pharmacol. Sci.* **25**, 358–365 (2004).
13. B. L. Gerhardstein, T. S. Puri, A. J. Chien, M. M. Hosey, Identification of the sites phosphorylated by cyclic AMP-dependent protein kinase on the β 2 subunit of L-type voltage-dependent calcium channels. *Biochemistry* **38**, 10361–10370 (1999).
14. T. J. Kamp, J. W. Hell, Regulation of cardiac L-type calcium channels by protein kinase A and protein kinase C. *Circ. Res.* **87**, 1095–1102 (2000).
15. K. S. De Jongh *et al*., Specific phosphorylation of a site in the full-length form of the α 1 subunit of the cardiac L-type calcium channel by adenosine 3′,5′-cyclic monophosphate-dependent protein kinase. *Biochemistry* **35**, 10392–10402 (1996).
16. M. D. Fuller, M. A. Emrick, M. Sadilek, T. Scheuer, W. A. Catterall, Molecular mechanism of calcium channel regulation in the fight-or-flight response. *Sci. Signal.* **3**, ra70 (2010).
17. J. Brandmayr *et al*., Deletion of the C-terminal phosphorylation sites in the cardiac β-subunit does not affect the basic β-adrenergic response of the heart and the Ca(v) 1.2 channel. *J. Biol. Chem.* **287**, 22584–22592 (2012).
18. T. Lemke *et al*., Unchanged β-adrenergic stimulation of cardiac L-type calcium channels in Ca_v 1.2 phosphorylation site S1928A mutant mice. *J. Biol. Chem.* **283**, 34738–34744 (2008).
19. L. Yang *et al*., β-adrenergic regulation of the L-type Ca^{2+} channel does not require phosphorylation of α_{1C} Ser1700. *Circ. Res.* **113**, 871–880 (2013).
20. G. Liu *et al*., Mechanism of adrenergic $Ca_V1.2$ stimulation revealed by proximity proteomics. *Nature* **577**, 695–700 (2020).
21. J. Miriyala, T. Nguyen, D. T. Yue, H. M. Colecraft, Role of CaVbeta subunits, and lack of functional reserve, in protein kinase A modulation of cardiac CaV1.2 channels. *Circ. Res.* **102**, e54–e64 (2008).
22. D. Roybal, J. A. Hennessey, S. O. Marx, The quest to identify the mechanism underlying adrenergic regulation of cardiac Ca^{2+} channels. *Channels (Austin)* **14**, 123–131 (2020).
23. S. Weiss, S. Oz, A. Benmocha, N. Dascal, Regulation of cardiac L-type Ca^{2+} channel CaV1.2 via the β-adrenergic-cAMP-protein kinase A pathway: Old dogmas, advances, and new uncertainties. *Circ. Res.* **113**, 617–631 (2013).
24. D. Singer-Lahat *et al*., Cardiac calcium channels expressed in Xenopus oocytes are modulated by dephosphorylation but not by cAMP-dependent phosphorylation. *Recept. Channels* **2**, 215–226 (1994).
25. P. Charnet, P. Lory, E. Bourinet, T. Collin, J. Nargeot, cAMP-dependent phosphorylation of the cardiac L-type Ca channel: A missing link? *Biochimie* **77**, 957–962 (1995).
26. E. Perez-Reyes, W. Yuan, X. Wei, D. M. Bers, Regulation of the cloned L-type cardiac calcium channel by cyclic-AMP-dependent protein kinase. *FEBS Lett.* **342**, 119–123 (1994).
27. N. Dascal, T. P. Snutch, H. Lübbert, N. Davidson, H. A. Lester, Expression and modulation of voltage-gated calcium channels after RNA injection in Xenopus oocytes. *Science* **231**, 1147–1150 (1986).
28. P. Lory, J. Nargeot, Cyclic AMP-dependent modulation of cardiac Ca channels expressed in *Xenopus laevis* oocytes. *Biochem. Biophys. Res. Commun.* **182**, 1059–1065 (1992).
29. S. Oz *et al*., Protein kinase A regulates C-terminally truncated Ca_V 1.2 in Xenopus oocytes: Roles of N- and C-termini of the α_{1C} subunit. *J. Physiol.* **595**, 3181–3202 (2017).
30. R. N. Correll, C. Pang, D. M. Niedowicz, B. S. Finlin, D. A. Andres, The RGK family of GTP-binding proteins: Regulators of voltage-dependent calcium channels and cytoskeleton remodeling. *Cell. Signal.* **20**, 292–300 (2008).
31. B. S. Finlin, S. M. Crump, J. Satin, D. A. Andres, Regulation of voltage-gated calcium channel activity by the Rem and Rad GTPases. *Proc. Natl. Acad. Sci. U.S.A.* **100**, 14469–14474 (2003).
32. T. Yang, H. M. Colecraft, Regulation of voltage-dependent calcium channels by RGK proteins. *Biochim. Biophys. Acta* **1828**, 1644–1654 (2013).
33. J. R. Manning *et al*., Rad GTPase deletion increases L-type calcium channel current leading to increased cardiac contraction. *J. Am. Heart Assoc.* **2**, e000459 (2013).
34. B. M. Ahern *et al*., Myocardial-restricted ablation of the GTPase RAD results in a pro-adaptive heart response in mice. *J. Biol. Chem.* **294**, 10913–10927 (2019).
35. A. Papa *et al*., Adrenergic $Ca_V1.2$ activation via Rad phosphorylation converges at α_{1C} I-II Loop. *Circ. Res.* **128**, 76–88 (2021).
36. S. Oz *et al*., Competitive and non-competitive regulation of calcium-dependent inactivation in $Ca_V1.2$ L-type Ca^{2+} channels by calmodulin and Ca^{2+}-binding protein 1. *J. Biol. Chem.* **288**, 12680–12691 (2013).
37. T. Yang, A. Puckerin, H. M. Colecraft, Distinct RGK GTPases differentially use α1- and auxiliary β-binding-dependent mechanisms to inhibit CaV1.2/CaV2.2 channels. *PLoS One* **7**, e37079 (2012).
38. Y. Opatowsky, C. C. Chen, K. P. Campbell, J. A. Hirsch, Structural analysis of the voltage-dependent calcium channel β subunit functional core and its complex with the α 1 interaction domain. *Neuron* **42**, 387–399 (2004).
39. P. Béguin *et al*., RGK small GTP-binding proteins interact with the nucleotide kinase domain of Ca^{2+}-channel β-subunits via an uncommon effector binding domain. *J. Biol. Chem.* **282**, 11509–11520 (2007).
40. Y. Blumenstein *et al*., A novel long N-terminal isoform of human L-type Ca2+ channel is up-regulated by protein kinase C. *J. Biol. Chem.* **277**, 3419–3423 (2002).
41. B. Dai, N. Saada, C. Echetebu, C. Dettbarn, P. Palade, A new promoter for α1C subunit of human L-type cardiac calcium channel Ca(V)1.2. *Biochem. Biophys. Res. Commun.* **296**, 429–433 (2002).
42. N. Kanevsky, N. Dascal, Regulation of maximal open probability is a separable function of Ca(v)β subunit in L-type Ca^{2+} channel, dependent on NH_2 terminus of α_{1C} (Ca(v)1.2α). *J. Gen. Physiol.* **128**, 15–36 (2006).
43. X. Wei *et al*., Modification of Ca^{2+} channel activity by deletions at the carboxyl terminus of the cardiac α_1 subunit. *J. Biol. Chem.* **269**, 1635–1640 (1994).
44. N. Gomez-Ospina, F. Tsuruta, O. Barreto-Chang, L. Hu, R. Dolmetsch, The C terminus of the L-type voltage-gated calcium channel Ca(V)1.2 encodes a transcription factor. *Cell* **127**, 591–606 (2006).
45. E. Schroder, M. Byse, J. Satin, L-type calcium channel C terminus autoregulates transcription. *Circ. Res.* **104**, 1373–1381 (2009).
46. V. A. Skeberdis, J. Jurevicius, R. Fischmeister, β-2 adrenergic activation of L-type Ca++ current in cardiac myocytes. *J. Pharmacol. Exp. Ther.* **283**, 452–461 (1997).
47. K. Kusano, R. Miledi, J. Stinnakre, Cholinergic and catecholaminergic receptors in the *Xenopus* oocyte membrane. *J. Physiol.* **328**, 143–170 (1982).
48. V. O. Nikolaev *et al*., β2-adrenergic receptor redistribution in heart failure changes cAMP compartmentation. *Science* **327**, 1653–1657 (2010).
49. P. T. Wright *et al*., Cardiomyocyte membrane structure and cAMP compartmentation produce anatomical variation in β_2AR-cAMP responsiveness in murine hearts. *Cell Rep.* **23**, 459–469 (2018).
50. S. M. Bryant, C. H. T. Kong, M. B. Cannell, C. H. Orchard, A. F. James, Loss of caveolin-3-dependent regulation of I_{Ca} in rat ventricular myocytes in heart failure. *Am. J. Physiol. Heart Circ. Physiol.* **314**, H521–H529 (2018).
51. M. J. Welsh *et al*., Cystic fibrosis transmembrane conductance regulator: A chloride channel with novel regulation. *Neuron* **8**, 821–829 (1992).
52. C. E. Bear *et al*., Cl- channel activity in *Xenopus* oocytes expressing the cystic fibrosis gene. *J. Biol. Chem.* **266**, 19142–19145 (1991).
53. Y. Uezono *et al*., Receptors that couple to 2 classes of G proteins increase cAMP and activate CFTR expressed in *Xenopus* oocytes. *Recept. Channels* **1**, 233–241 (1993).
54. P. Chidiac, T. E. Hebert, M. Valiquette, M. Dennis, M. Bouvier, Inverse agonist activity of β-adrenergic antagonists. *Mol. Pharmacol.* **45**, 490–499 (1994).
55. K. N. M. Man, P. Bartels, M. C. Horne, J. W. Hell, Tissue-specific adrenergic regulation of the L-type Ca^{2+} channel $Ca_V1.2$. *Sci. Signal.* **13**, eabc6438 (2020).
56. T. Perets, Y. Blumenstein, E. Shistik, I. Lotan, N. Dascal, A potential site of functional modulation by protein kinase A in the cardiac Ca^{2+} channel α_{1C} subunit. *FEBS Lett.* **384**, 189–192 (1996).
57. M. B. Clark *et al*., Long-read sequencing reveals the complex splicing profile of the psychiatric risk gene CACNA1C in human brain. *Mol. Psychiatry* **25**, 37–47 (2020).
58. Z. Z. Tang *et al*., Transcript scanning reveals novel and extensive splice variations in human l-type voltage-gated calcium channel, Cav1.2 alpha1 subunit. *J. Biol. Chem.* **279**, 44335–44343 (2004).
59. M. Biel *et al*., Primary structure and functional expression of a cyclic nucleotide-gated channel from rabbit aorta. *FEBS Lett.* **329**, 134–138 (1993).
60. T. P. Snutch, W. J. Tomlinson, J. P. Leonard, M. M. Gilbert, Distinct calcium channels are generated by alternative splicing and are differentially expressed in the mammalian CNS. *Neuron* **7**, 45–57 (1991).
61. E. Tareilus *et al*., A *Xenopus* oocyte β subunit: Evidence for a role in the assembly/expression of voltage-gated calcium channels that is separate from its role as a regulatory subunit. *Proc. Natl. Acad. Sci. U.S.A.* **94**, 1703–1708 (1997).
62. K. Chakir *et al*., The third intracellular loop and the carboxyl terminus of β2-adrenergic receptor confer spontaneous activity of the receptor. *Mol. Pharmacol.* **64**, 1048–1058 (2003).
63. S. J. Zhang *et al*., Inhibition of spontaneous β 2-adrenergic activation rescues β 1-adrenergic contractile response in cardiomyocytes overexpressing β 2-adrenoceptor. *J. Biol. Chem.* **275**, 21773–21779 (2000).
64. J. L. Sanchez-Alonso *et al*., Microdomain-specific modulation of L-type calcium channels leads to triggered ventricular arrhythmia in heart failure. *Circ. Res.* **119**, 944–955 (2016).
65. J. L. Sanchez-Alonso *et al*., Nanoscale regulation of L-type calcium channels differentiates between ischemic and dilated cardiomyopathies. *EBioMedicine* **57**, 102845 (2020).
66. H. Qian *et al*., Phosphorylation of Ser1928 mediates the enhanced activity of the L-type Ca^{2+} channel $Ca_v1.2$ by the β2-adrenergic receptor in neurons. *Sci. Signal.* **10**, eaaf9659 (2017).
67. M. A. Nystoriak *et al*., Ser^{1928} phosphorylation by PKA stimulates the L-type Ca^{2+} channel $Ca_V1.2$ and vasoconstriction during acute hyperglycemia and diabetes. *Sci. Signal.* **10**, eaaf9647 (2017).
68. A. N. Ganesan, C. Maack, D. C. Johns, A. Sidor, B. O'Rourke, β-adrenergic stimulation of L-type Ca^{2+} channels in cardiac myocytes requires the distal carboxyl terminus of α_{1C} but not serine 1928. *Circ. Res.* **98**, e11–e18 (2006).
69. A. Folci *et al*., Molecular mimicking of C-terminal phosphorylation tunes the surface dynamics of $Ca_V1.2$ calcium channels in hippocampal neurons. *J. Biol. Chem.* **293**, 1040–1053 (2018).
70. T. Pallien, E. Klussmann, New aspects in cardiac L-type Ca^{2+} channel regulation. *Biochem. Soc. Trans.* **48**, 39–49 (2020).
71. R. Hullin *et al*., Calcium channel β subunit heterogeneity: Functional expression of cloned cDNA from heart, aorta and brain. *EMBO J.* **11**, 885–890 (1992).
72. S. Weiss *et al*., Modulation of distinct isoforms of L-type calcium channels by $G(_q)$-coupled receptors in *Xenopus* oocytes: Antagonistic effects of Gβγ and protein kinase C. *Channels (Austin)* **6**, 426–437 (2012).
73. Y. Opatowsky, O. Chomsky-Hecht, M. G. Kang, K. P. Campbell, J. A. Hirsch, The voltage-dependent calcium channel β subunit contains two stable interacting domains. *J. Biol. Chem.* **278**, 52323–52332 (2003).
74. Y. Sasson, L. Navon-Perry, D. Huppert, J. A. Hirsch, RGK family G-domain:GTP analog complex structures and nucleotide-binding properties. *J. Mol. Biol.* **413**, 372–389 (2011).